

The all-angle self-collimating phenomenon in photonic crystals with rectangular symmetry

Yi Xu, Xiao-Jun Chen, Sheng Lan, Qi Guo, Wei Hu and Li-Jun Wu¹

Laboratory of Photonic Information Technology, School for Information and Optoelectronic Science and Engineering, South China Normal University, Guangzhou 510006, People's Republic of China

E-mail: ljwu@sncu.edu.cn

Received 10 May 2008, accepted for publication 12 June 2008

Published 1 July 2008

Online at stacks.iop.org/JOptA/10/085201

Abstract

We propose a two-dimensional photonic crystal of rectangular symmetry with rather straight iso-frequency lines over the whole first Brillouin zone along the ΓX direction to realize all-angle self-collimation. By tracking the spatial evolution and transmission efficiency of the collimated beam along the propagating direction, it is found that the beam spreading and propagation loss are negligible for incident angles within $\pm 85^\circ$. The self-collimating behaviors in the rectangular and square lattices are compared and the differences between them are investigated. As an application, a Y-shaped beam splitter with transmission efficiencies for both branches as high as 43.8% is constructed by combining two rotated rectangular structures.

Keywords: photonic crystal, self-collimation, rectangular lattice

(Some figures in this article are in colour only in the electronic version)

1. Introduction

Photonic crystals (PhCs) [1] have attracted a lot of attention in the last two decades due to their ability to control the flow of light. To realize their functionalities such as ultracompact wavelength-selective, guiding and routing components on a miniature scale, it is necessary to precisely control the spatial profile of light propagation through PhC lattices [2–4].

The propagation of light in a PhC is governed by its dispersion surfaces, which characterize the relationship between the frequency of the wave ν and its associated wavevector \mathbf{k} . By analyzing the cross section of the dispersion surface at a given frequency, equi-frequency contours (EFCs) can be obtained (through the plane wave expansion (PWE) method). The direction of light propagation in the structure is then given by the group velocity $v_g = \nabla_{\mathbf{k}}\omega(\mathbf{k})$, which is perpendicular to these contours. Basically, the so-called self-collimating or self-guiding phenomenon occurs where the EFC is flat [5–10]. When such a mode is excited, the light

propagates in PhCs without diffraction, i.e. a narrow beam could propagate in PhCs with negligible spreading. In this way, the spatial profile of the light could be controlled effectively. This behavior was initially demonstrated by Kosaka *et al* [9] and Wu *et al* [10] in three-dimensional (3D) and two-dimensional (2D) PhCs, respectively.

It has been known that the collimating efficiency is dependent on the angular collimating range, and a PhC with a wide collimating range is highly desirable. In principle, there are two ways to expand this range. One is to shrink the EFC of the uniform incident medium by changing the incident materials. As a result, more incoming k -vectors will be included within the flat EFC part of the PhC. This is similar to what happens in the all-angle negative refraction [11]. However, this method is limited by the choice of the incident materials since it is difficult to obtain a dielectric material with refractive index less than 1. Air is the most commonly used incident material because of its relatively small circular EFC. Another method to expanding the angular collimating range is to lower the symmetry of

¹ Author to whom any correspondence should be addressed.

the photonic structure. For example, the four-fold symmetry square lattice has a larger angular collimating range than the six-fold hexagonal structure. Therefore, most studies on the self-guiding phenomenon have concentrated on square geometries [5–8]. Intuitively, by lowering the symmetry further it would be possible to increase the angular collimating range. For example, Ogawa *et al* recently demonstrated a light-focusing device using PhCs with a 2D parallelogram lattice. They achieved a wide-angle collimation by breaking the $\pi/2$ rotation symmetry (four-fold symmetry) of the square structure in the first band [12]. In fact, light can be self-collimated both in the first (ΓM direction) and second (ΓX) bands of a square lattice. The equi-frequency squares, however, are both rounded at the corners for these two bands. Consequently, not all the incident angles could be collimated and a longer part of the flat EFC is necessary to achieve a wider angular collimating range. For some frequencies, the shape of the EFC mimics the shape of the first Brillouin zone (FBZ). In such a case, a wider real space will correspond to a narrower reciprocal space (FBZ), where a longer part of flat EFC is easier to be obtained. In this paper, we propose to lower the symmetry of the square lattice and thus modify the shape of the FBZ to increase the angular collimating range.

2. The all-angle self-collimating phenomenon

We apply a rectangular lattice, which was originally proposed to improve the transmission efficiency in the Superprism effect [13], to realize an all-angle self-collimation. An extra parameter, the ratio β of the longer lattice vector b over the shorter one a , is introduced to characterize the distortion from the square lattice. Comparing with the higher symmetrical square lattice, the rectangular one has more structure parameters to tune and offers us more flexibility to tailor the shape of the BZ.

The basic structure is constructed by arranging dielectric rods ($n = 3.21$) in air to form a rectangular geometry. The radius of the dielectric rod is $r = 0.15a$. Here the transverse-magnetic (TM) wave with electric field parallel to the rods will be studied. A freely distributed software package [14] was employed to obtain the fully vectorial eigenmodes solution of Maxwell's equations. In order to investigate its influence on the self-collimation, β has been scanned from 1 to 2.5 (with a fixed) with an increment of 0.1 by monitoring the evolution of band surfaces and EFCs. Figure 1(a) displays four typical band surfaces. Obviously, $\beta = 1$ corresponds to a square lattice and the band surface possesses a square symmetry. With increasing β , the band surface shrinks in the direction where the reciprocal lattice shrinks (the real lattice expands). Meanwhile, the centers of the two wings sink and the ends hump. Further increasing the β leads to some connections between the wing-ends and the central part of the band surface. When $\beta \geq 1.9$, a planar part of the band surface emerges at some frequencies, implying that the EFC is becoming flat. As $\beta \geq 2.1$, however, the modulation from the PhC starts to be weak due to the small filling factor of the dielectric material in the structure. As a result, the confinement of the directional gap (along the ΓX direction) becomes weak and the light

leaks to the ΓX direction, which will affect the collimating efficiency (details of the directional gap will be addressed in the following). Therefore, infinitely compressing the FBZ from one direction makes no sense. We then choose β to be 2 to demonstrate wide-angle self-collimation. Figure 1(b) describes the corresponding EFCs. The FBZ is marked by gray dashed lines. Remarkably, the EFC becomes significantly flat when the normalized frequency $\nu = a/\lambda$ approaches $0.468 c/a$, where c is the speed of the light. In this case, even when the incident angle is 90° , the propagation direction in the PhCs could still be collimated along the $\Gamma X'$ direction as indicated by the bold gray arrow. Therefore, all azimuth angles within $\pm 90^\circ$ could be collimated by this rectangular structure. It is worth noting that 'all-angle self-collimation' here is only applicable for plane waves (single k -vectors). When a Gaussian beam with a spread of k -vectors enters into the PhC structure at 90° incident angle, k -vectors with angles larger than 90° will not be collimated.

3. Self-collimation for incident angle 85°

So far, we have revealed the principal of the all-angle self-collimating phenomenon in PhCs with rectangular lattices. In this part, we will demonstrate the self-collimating phenomenon for an incident angle as large as 85° by numerical simulations based on the finite-difference time-domain (FDTD) technique, which is more intuitive and accurate than the PWE method. To do so, a Gaussian beam with a width of $3a$ is launched into the PhC from air at 85° . Spatial evolution of the beam in PhCs is presented in figure 2(a). As expected, the beam is collimated along the $\Gamma X'$ direction and does not spread even after propagating a distance as long as $200a$. To demonstrate the quantitative results, we calculated the sums of electric field's Fourier coefficients, which are evaluated over the last simulation period (referred to the source) at a certain grid point. Therefore, these sums can be thought of as a type of time average. The E -field amplitudes along the propagating direction can then be obtained by connecting the sums at every single spatial grid, as shown in figure 2(b). It can be seen the maxima of the field component E_z are almost identical, implying that the propagation loss of the collimated beam in the PhCs is negligible. Therefore, incident angles at least within $\pm 85^\circ$ can be collimated along the $\Gamma X'$ direction (we did not try incident angles between 86° and 90° because of their large inclination). Limited by computer power, we did not try structures longer than $200a$. From the trend in figure 2(b), we believe that the propagation loss will still be very small even after longer propagating distance.

4. Differences in self-collimation between rectangular and square structures

One significant difference of the self-collimating phenomenon between these two structures is the existence of the directional gap in the rectangular structure. From figure 1(b) it can be seen that there is no mode existing along the ΓX direction, suggesting that this direction is in the band gap at the corresponding frequencies. In contrast, for a square lattice,

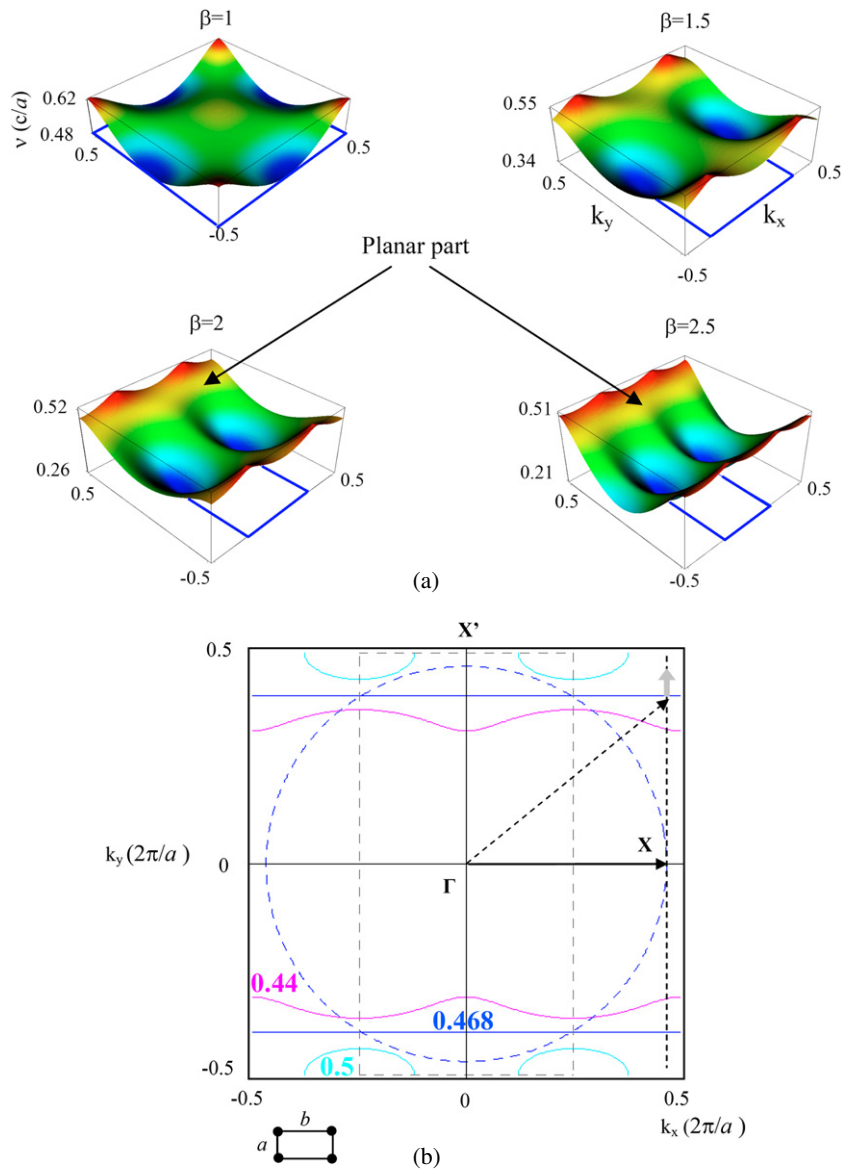


Figure 1. (a) Band surfaces of the second branch with different ratio $\beta = b/a$. The bold blue frames correspond to the first Brillouin zone. All the x and y axes are for $k_x(2\pi/a)$ and $k_y(2\pi/a)$, while z is for $v = a/\lambda$. (b) EFCs for the rectangular lattice with $\beta = 2$. The black solid arrow represents the incident k -vector for incident angle 90° in air while the black dashed arrow represents the k -vector in PhCs. The blue dashed circle is EFC for air at a frequency of $0.468c/a$. The propagating direction in PhCs is shown as in the bold gray arrow.

the EFCs are closed loops and there are modes for all the four directions in the second branch at some typical collimating frequencies. Figure 3(b₂) shows one of these loops at a frequency of $0.552c/a$ (we borrowed the structure parameters from [6]; the refractive index of the rods is set the same as in this paper). The advantage of this directional gap in the rectangular structure is that the light will have no chance to escape along the ΓX direction during the propagation. Thus, the transmission along the collimating direction could be improved. This point can be easily verified by FDTD simulations, as shown in figures 3(a₁) and (b₁). Point sources are introduced into the centers of the rectangular and square structures to cover all directions of k -vectors at a certain frequency. In the former structure, all the light is guided along the vertical direction and almost no light leaks to the horizontal

direction. For the latter case, however, the light propagates along the vertical and horizontal directions equally.

Another difference that needs to be addressed is the coupling from Bloch modes to air modes. In the rectangular structure, the propagating waves of the point source (the evanescent waves from the point source are beyond the scope of this paper) could excite continuous propagating Bloch modes along the flat EFC at the collimating frequency. These excited Bloch modes have the same propagating direction in the PhCs. When they exit from PhCs into air, corresponding k -vectors for the output beam will be recovered without any gap as the EFC is continuously flat. As a result, a ‘point’ image emerges at the output interface, as shown in figure 3(a₁). Correspondingly, the pink-shaded region (which schematically denotes the output modes in air at the upper PhC–air interface)

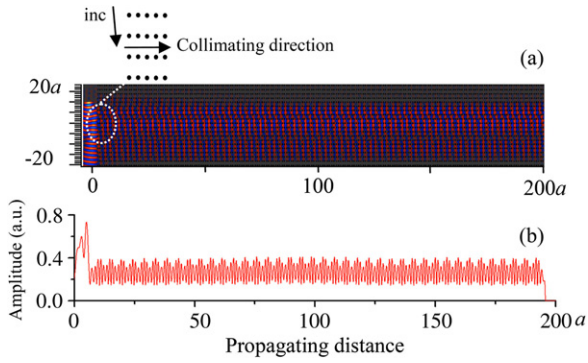


Figure 2. (a) The spatial evolution of a beam incident from air into rectangular PhCs at 85° (incident from left to right). The top inset displays the incident interface, incident, and collimated directions schematically. (b) Time average of the E_z component after different propagating distance. The oscillation of E_z is due to the modulation of the periodic PhC.

in figure 3(a₂) is a continuum. In the case of a square lattice, however, the pink-shaded region is separated into three parts because of the broken flat EFC, as shown in the gray twill weave in figure 3(b₂). Three consequently separated components are also observable by FDTD simulation, as shown in figure 3(b₁).

5. Y-shaped beam splitter

Apart from acting as a self-collimator, this rectangular structure could also be used to construct some useful circuits such as Y-shaped beam splitters with high transmission

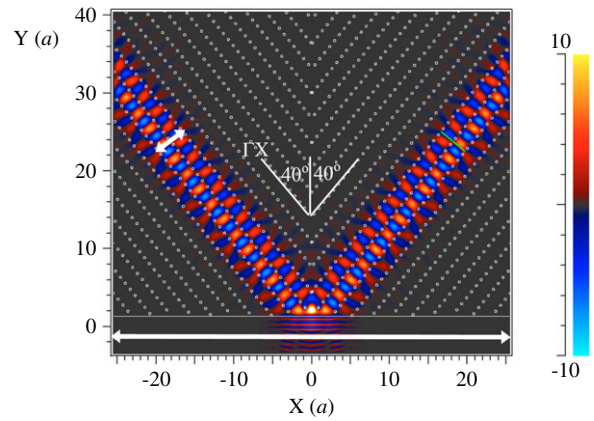


Figure 4. Field distributions for the Y-shaped beam splitter. The splitter is constructed by binding two rotated (40° rotation away from ΓX) rectangular lattices together with mirror symmetry. The incident beam width is $6a$. Bold white double arrows describe the positions and lengths of the power monitors.

because of its high coupling efficiency at large incident angles. For example, we can bind two rectangular lattices, which are rotated by 40° along the vertical direction, with mirror symmetry to construct a device as illustrated in figure 4. Several rods have been removed at the input port to improve the coupling efficiency. At a frequency of $0.468c/a$, the transmitted power of each branch reaches about 43.8% (normalized to the incident power). It is important to note that the transmitted powers at various positions of the two branches are almost constant, suggesting that the propagation loss of the Y-shaped beam splitter is negligible. This is similar

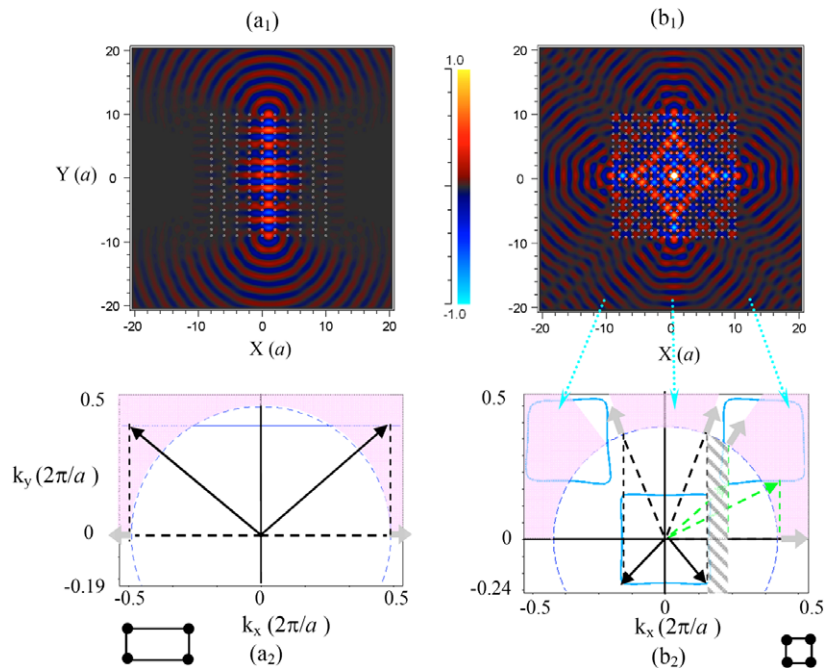


Figure 3. Field distributions ((a₁), (b₁)) and EFCs ((a₂), (b₂)) for rectangular and square lattices at the typical collimating efficiencies $0.468c/a$ and $0.552c/a$, respectively. In FDTD simulations, point sources are located at the center of the structures. Solid black and green dashed arrows are for k -vectors in PhCs while bold gray arrows are for group velocities in air. All the vertical dashed lines stand for the k -vector conservation lines, which are perpendicular to input interfaces.

to that shown in figure 2(b). Therefore, this beam splitter is very useful when long distance transmission is required in the circuits. The reflection is found to be around 12.1%. The remaining 0.3% power corresponds to the scattering loss out of the range of the power monitors with finite width, which are shown in green lines in figure 4.

6. Conclusions

In summary, we have proposed a rectangular 2D PhC structure to provide rather flat EFCs across the whole FBZ along the ΓX direction. The all-angle self-collimating phenomenon has been observed in this structure. By tracking the spatial evolution and transmission efficiency of the collimated beam after different propagating distance, it is found that its spreading and propagation loss are negligible for incident angles within $\pm 85^\circ$. The differences of the self-collimation between the rectangular and square lattices have been studied. Finally, a Y-shaped beam splitter has been constructed by combining two parts of the rotated rectangular structures. Transmission efficiencies for both branches as high as 43.8% have been achieved.

Acknowledgments

The authors acknowledge the financial support from the National Natural Science Foundation of China (Grant No. 10774050) and the Program for Innovative Research Team of the Higher Education in Guangdong (Grant No. 06CXTD005). One of the authors (S Lan) is grateful for the financial support by the Program for New Century Excellent Talents (NCET) in University of China.

References

- [1] Yablonovitch E 1987 Inhibited spontaneous emission in solidstate physics and electronics *Phys. Rev. Lett.* **58** 2059–62
- [2] Kosada H, Kawashima T, Tomita A, Notomi M, Tamamura T, Sato T and Kawakami S 1998 Superprism phenomena in photonic crystals *Phys. Rev. B* **58** 10096–9
- [3] Wu L, Mazilu M, Karle T and Krauss T F 2002 Superprism phenomena in planar photonic crystals *IEEE J. Quantum Electron.* **38** 915–8
- [4] Wu L, Mazilu M, Gallet J-F and Krauss T F 2005 Dual lattice photonic-crystal beam splitters *Appl. Phys. Lett.* **86** 211106–9
- [5] Witzens J, Loncar M and Schere A 2002 Self-collimation in planar photonic crystals *IEEE J. Sel. Top. Quantum Electron.* **8** 1246–57
- [6] Chigrin D N, Enoch S, Torres C M S and Tayeb G 2003 Self-guiding in two-dimensional photonic crystals *Opt. Express* **11** 1203–11
- [7] Rakich P T, Dahlem M S, Tandon S, Ibanescu M, Soljačić M, Petrich G S, Joannopoulos J D, Kolodziejski L A and Ippen E P 2006 Achieving centimeter-scale supercollimation in a large-area two-dimensional photonic crystal *Nat. Mater.* **5** 93–6
- [8] Prather D W, Shi S, Murakowski J, Schneider G J, Sharkawy A, Chen C, Miao B and Martin R 2007 Self-collimation in photonic crystal structures: a new paradigm for applications and device development *J. Phys. D: Appl. Phys.* **40** 2635–51
- [9] Kosaka H, Kawashima T, Tomita A, Notomi M, Tamamura T, Sato T and Kawakami S 1999 Self-collimating phenomena in photonic crystals *Appl. Phys. Lett.* **74** 1212–4
- [10] Wu L, Mazilu M and Krauss T F 2003 Beam steering in planar-photonic crystals: from superprism to supercollimator *J. Lightwave Technol.* **21** 561–6
- [11] Luo C, Johnson S G, Joannopoulos J D and Pendry J B 2002 All-angle negative refraction without negative effective index *Phys. Rev. B* **65** 201104–6(R)
- [12] Ogawa Y, Omura Y and Iida Y 2005 Study on self-collimated light-focusing device using the 2D photonic crystal with a parallelogram lattice *J. Lightwave Technol.* **23** 4374–81
- [13] Căbuz A I, Centeno E and Cassagne D 2004 Superprism effect in bidimensional rectangular photonic crystals *Appl. Phys. Lett.* **84** 2031–3
- [14] Johnson S G and Joannopoulos J D 2001 Block-iterative frequency-domain methods for Maxwell's equations in a planewave basis *Opt. Express* **8** 173–90 <http://www.opticsexpress.org/abstract.cfm?URI=OPEX-8-3-173>